ELSEVIER

www.elsevier.nl/locate/jorganchem

Journal of Organometallic Chemistry 598 (2000) 381–386

Journal of Organometallic Chemistry

Monoorganotin–polyoxometal compounds

Part 1. Synthesis and crystal structure of $[(^{i}PrSn)_{11}(V^{IV}O)O_{14}(OH)_6]Cl{\cdot}2DMF{\cdot}H_2O$. The first example in a series of monoorganotin–polyoxometal compounds with icosahedral metal arrangement and various contents of tin and vanadium

Guido Kastner, Hans Reuter *

Universität Osnabrück, Institut für Chemie, Anorganische Chemie II, Barbarastr. 7, D-49069 Osnabrück, Germany

Received 9 August 1999; accepted 22 November 1999

Abstract

The synthesis, molecular and crystal structure of the $[(^{i}PrSn)_{11}(VO)O_{14}(OH)_6]^{+}$ ion **1** are described. **1** was found in the compound **1**$\cdot Cl\cdot 2DMF\cdot H_2O$ and is the first oxovanadium derivative of the long-known $[(^{i}PrSn)_{12}O_{14}(OH)_6]^{2+}$ ion **2**. The green compound crystallizes in the triclinic space group $P\bar{1}$ with $a = 13.989(2)$, $b = 14.541(2)$, $c = 19.713(3)$ Å, $\alpha = 97.16(1)°$, $\beta = 93.79(1)°$, $\gamma = 116.08(1)°$, $V = 3540.5(9)$ Å^3, $Z = 2$. **1** shows the same icosahedral arrangement of metal atoms as the tin compound as well as the same arrangement of oxygen atoms. The vanadium atom is coordinated by five oxygen atoms and replaces one of the square-pyramidally coordinated organotin groups. In the solid state the big cations are linked by hydrogen bonds to Cl^{-} ions forming chains along the *a* axis. Two of these chains are linked by $OH\cdots O{=}V$ hydrogen bonds resulting in a band structure. © 2000 Elsevier Science S.A. All rights reserved.

Keywords: Tin; Vanadium; Heteropolyoxometalates; Cage ion; Crystal structure

---

1. Introduction

The formation of polyoxometal compounds (anions as well as cations) is widespread through the elements of the periodic table. In recent times, however, the interest of chemists has focused mostly on the polyoxometalates of the early transition elements because of the enormous variety of structural types they form accompanied by interesting catalytical properties that give rise to a lot of possible applications [1]. In contrast to these elements, metals of the p-block are characterized more often by the formation of isopolyoxometal cations well established, for example, for Al, Bi and Sn [2]. This area is widened by the fact that monoorganotin halides $RSnX_3$ (X = Cl, Br, I) and their hydrolysis products behave in many aspects like naked metal atoms, forming highly nucleated isopolyoxotin cations such as $[(RSn)_{12}O_{14}(OH)_6]^{2+}$ [3; R = *i*Pr] [4,5,6; R = Bu] or heteropolyoxo cations such as $[Na \subset (^{i}PrSn)_{12}O_4(OH)_{24}]^{3+}$ [7].

This chemistry is possible due to the low tendency of the carbon–tin bond to hydrolyze, so that a potential coordination site at tin is blocked by an apolar organic moiety with the effect that the tin–oxygen framework of the polyoxometal compound is stabilized by an apolar shell.

In the last few years some effort has been made to incorporate tin or organotin compounds within polyoxometalates of Mo or W. Chorghade and Pope prepared and characterized several kinds of tungstostannates(II) of the Keggin and Dawson types [8] as well as a number of tris(organotin) Keggin tungstosilicates con-

---

* Corresponding author. Tel.: +49-541-9692778; fax: +49-541-9692370.

E-mail address: hreuter@rz.uni-osnabrueck.de (H. Reuter)

PII: S0022-328X(99)00738-X

taining anions like $[(\mathrm{PhSn})_3(\beta\text{-}\mathrm{SiW}_9\mathrm{O}_{37})]^{7-}$ or $[(\mathrm{PhSnOH})_3(\alpha\text{-}\mathrm{SiW}_9\mathrm{O}_{34})_2]^{15-}$ [9]. Krebs et al. prepared a compound containing the $[(\mathrm{Ph}_2\mathrm{Sn})_2[\mu\text{-}\mathrm{OH})_2[\mu\text{-}\mathrm{MoO}_4)_2]^{2-}$ anion [10], the first example of organotin molybdates showing isolated organotin oxomolybdenum ions. On the other hand, polymeric structures were found in $[\mathrm{Me}_2\mathrm{SnMoO}_4]$ [11] or $[(\mathrm{Me}_3\mathrm{Sn})_2\mathrm{MoO}_4]$ [12]. All these compounds are mainly characterized by a low degree of substitution of the early transition elements by tin.

Our interest in this area was focused on synthetic and structural chemical aspects. The structure of the $[({}^i\mathrm{PrSn})_{12}\mathrm{O}_{14}(\mathrm{OH})_6]^{2+}$ ion **2** shown in Fig. 1 is characterized by a central six-membered ring of square-pyramidally coordinated $\{\mathrm{RSnO}_4\}$ units which is capped at both sides by three edge-sharing $\{\mathrm{RSnO}_5\}$ octahedra. The same structure is adopted by the anion $[(\mathrm{VO})_{12}\mathrm{O}_{12}\mathrm{F}_2(\mathrm{OH})_6]^{6-}$ that was prepared by Müller et al. [13], with the fluorine atoms directed inside the VO cage. For us, it was of interest to see whether it is possible for a VO group to substitute a RSn group either in the square-pyramidal or octahedral sites of molecules derived from the icosahedral metal arrangement found in **2** and to find out synthetic ways to realize that substitution.

To our surprise many different experimental routes realize the subtitutions, and indeed, X-ray crystallography studies showed that VO can replace RSn giving rise to compounds with one, two, three, or six VO groups in the positions of the square-pyramidally coordinated organotin groups in **2** with icosahedral metal arrangement. Here we report the synthesis and crystal structure of the $[({}^i\mathrm{PrSn})_{11}(\mathrm{VO})\mathrm{O}_{14}(\mathrm{OH})_6]^+$ ion **1**, which could be isolated in the compound **1**·Cl·2DMF·$\mathrm{H_2O}$. This is the first example in a series of monoorganotin polyoxometal compounds with icosahedral metal arrangement and various contents of tin and vanadium. The other compounds still are subject to further investigation, mainly because of their great instability (see below).

2. Experimental

2.1. Synthesis

A total of 0.5 g of ${}^i\mathrm{PrSn(OH)_2Cl}\cdot0.75\mathrm{H_2O}$ [for synthesis see Ref. 3] (2.04 mmol), 0.15 ml of ethylenediamine (0.17 g, 2.8 mmol) and an excess of $\mathrm{VOSO_4}\cdot5\mathrm{H_2O}$ (0.1 g, 0.41mmol) were added to 30 ml of *N*,*N*-dimethylformamide. This suspension was stirred at room temperature for 24 h. During this time most of the compounds dissolved and the liquid turned green. The solution was filtered off from undissolved material into a crystallization vessel and the solvent was left to evaporate. Within several days, green needle-shaped crystals of **1**·Cl·2DMF·$\mathrm{H_2O}$ appeared. Although these crystals are stable for several days within the mother liquor, they decompose within several minutes outside the mother liquor due to the loss of solvent molecules.

Yield: about 0.3 g/1.4 mmol, 68% (based on tin).

2.2. X-ray crystallography

A single crystal of **1**·Cl·2DMF·$\mathrm{H_2O}$ (dimensions $0.4 \times 0.2 \times 0.2$ mm^3) was placed in a sealed Lindemann capillary for indexing and intensity data collection on a Siemens P4 four-circle diffractometer with a sealed-tube Mo–K$_\alpha$ X-ray source ($\lambda = 0.71073$ Å) and a graphite monochromator. The measurement was carried out at ambient temperature (298 K). The unit cell was refined from 42 reflections in the range of $8.2 \leq \theta \leq 25°$. A total of 7388 reflections was collected in a range of $1.74 \leq \theta \leq 22.03°$ giving 6282 independent reflections ($R_\mathrm{int} = 0.0272$). Three standard reflections were mea-

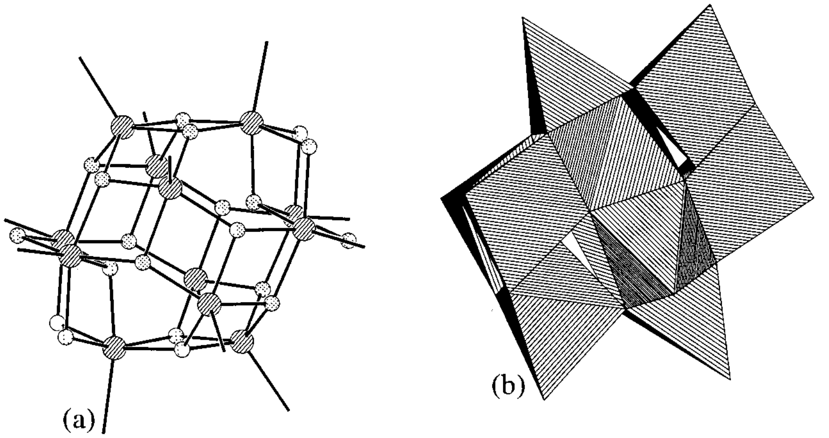

Fig. 1. (a) Ball-and-stick model of the metal–oxygen framework found in the $[(\mathrm{RSn})_{12}\mathrm{O}_{14}(\mathrm{OH})_6]^{2+}$ ion and the $[(\mathrm{VO})_{12}\mathrm{O}_{12}\mathrm{F}_2(\mathrm{OH})_6]^{6-}$ ion, in which the two oxygen atoms directed towards the inside of the cage are replaced by flourine. Metal atoms (M = Sn or V) are represented as dashed circles, (O or F) as dotted circles. Positions of the outer moieties (R or O) are indicated by their bonds. (b) The same structure type shown as polyhedra model.

Table 1
Crystal data and structure refinement for $[(^i\mathrm{PrSn})_{11}(\mathrm{VO})\mathrm{O}_{14}(\mathrm{OH})_6]\mathrm{Cl}\cdot 2\mathrm{DMF}\cdot \mathrm{H_2O}$

Empirical formula	$C_{39}H_{99}ClN_2O_{24}Sn_{11}V$
Formula weight	2372.18
Temperature (K)	293(2)
Wavelength (Å)	0.71073
Crystal system	Triclinic
Space group	$P\bar{1}$ (no. 2)
Unit cell dimensions	
a (Å)	13.989(2)
b (Å)	14.541(2)
c (Å)	19.713(3)
α (°)	97.16(1)
β (°)	93.79(1)
γ (°)	116.08(1)
Volume (Å^3)	3540.5(9)
Z	2
$D_{\mathrm{calc.}}$ (Mg m^{-3})	2.225
Absorption coefficient (mm^{-1})	4.034
$F(000)$	2258
Crystal size (mm^3)	$0.4 \times 0.2 \times 0.2$
Theta range for data collection (°)	1.74–22.03
Index ranges	$-1 \le h \le 14$, $-15 \le k \le 13$, $-20 \le l \le 20$
Reflections collected	7388
Independent reflections	6282 [$R_{\mathrm{int}} = 0.0272$]
Refinement method	Full-matrix least-squares on F^2
Data/restraints/parameters	6282/11/484
Goodness-of-fit on F^2	1.046
Final R indices [$I > 2\sigma(I)$]	$R_1 = 0.0595$, $wR_2 = 0.1278$
Final R indices (all data)	[a]$R_1 = 0.0851$, [b]$wR_2 = 0.1397$
Largest difference peak and hole (e Å^{-3})	0.981 and -0.733

[a] $R_1 = \Sigma(|F_o| - |F_c|)/\Sigma|F_o|$.
[b] $wR_2 = [\Sigma w(F_o^2 - F_c^2)^2)/\Sigma w(F_o^2)^2]^{1/2}$.

sured every 100 reflections showing a decay of over 50% during data collection. Besides the normal data reduction, an intensity correction was applied but no absorption correction. The structure was solved by standard direct methods and refined from successive difference Fourier syntheses. The final cycle of refinement, including the atomic coordinates (all non-H atoms, H-atoms fixed), anisotropic thermal parameters (all Sn, V, Cl atoms and O atoms of the cage ion) and isotropic thermal parameters (all C and N atoms, O atoms of the solvent molecules and one common isotropic thermal parameter for all H atoms) converged at $R_1 = 0.0595$, $wR_2 = 0.1278$ [$I > 2\sigma(I)$]. In the final difference Fourier map the largest peak and hole were 0.981 and -0.733 e Å^{-3}, respectively. Further crystallographic data are summarized in Table 1. Structure solution and refinement were carried out using the SHELXTL program package [14].

3. Results and discussion

There are two formula units in the unit cell and because the multiplicity in the triclinic space group $P\bar{1}$ is two, the asymmetric unit consists of one acentric $[(^i\mathrm{PrSn})_{11}(\mathrm{VO})\mathrm{O}_{14}(\mathrm{OH})_6]^+$ ion **1**, one Cl^- ion, two DMF molecules and one $\mathrm{H_2O}$ molecule.

The characteristic building unit of the crystal structure is the cage ion **1**. Therein, two trimeric, edge-sharing $\{^i\mathrm{PrSnO}_5\}$ octahedra are linked by a ring of five square-pyramidally coordinated $\{^i\mathrm{PrSnO}_4\}$ units and one square-pyramidally coordinated $\{\mathrm{OVO}_4\}$ unit (see Fig. 2). The metal atoms are arranged in the form of a

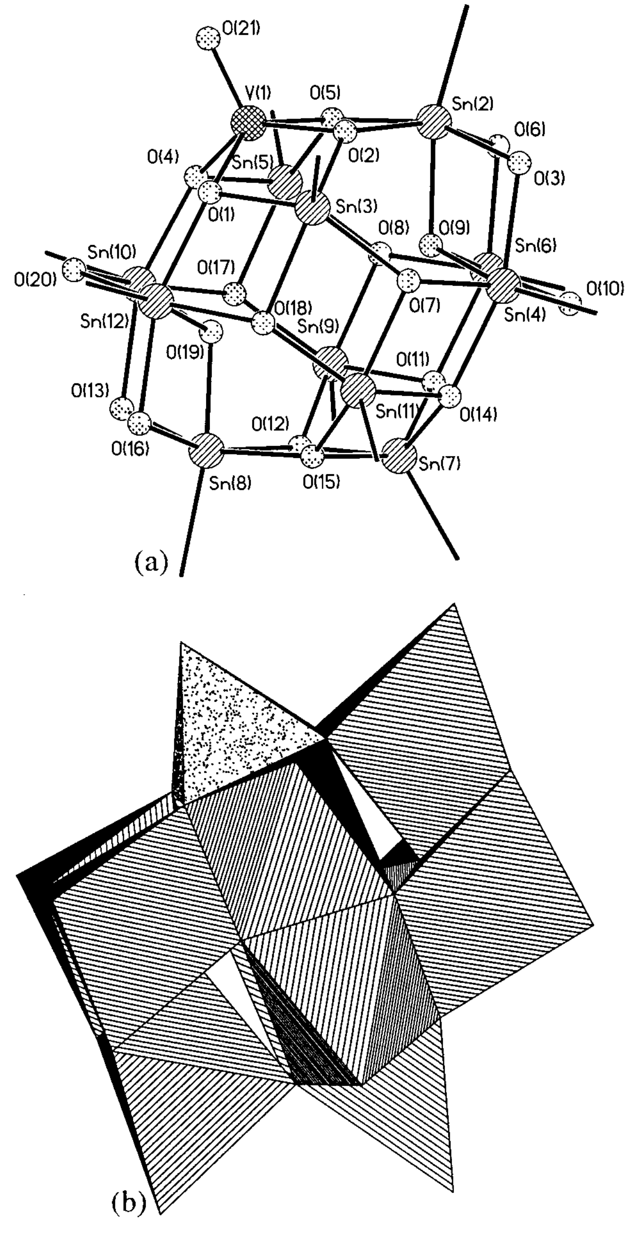

Fig. 2. (a) Ball-and-stick- representation of $[(^i\mathrm{PrSn})_{11}(\mathrm{VO})\mathrm{O}_{14}(\mathrm{OH})_6]^+$ showing the atomic numbering scheme. Tin atoms are represented as dashed circles, the vanadium atom as a cross-hatched circle and the oxygen atoms as dotted circles. The isopropyl groups are omitted for clarity but their position is shown by their Sn–C bonds. (b) The same structure shown as polyhedra model, octahedra and square pyramids around tin atoms are dashed, the square pyramid around vanadium, dotted.

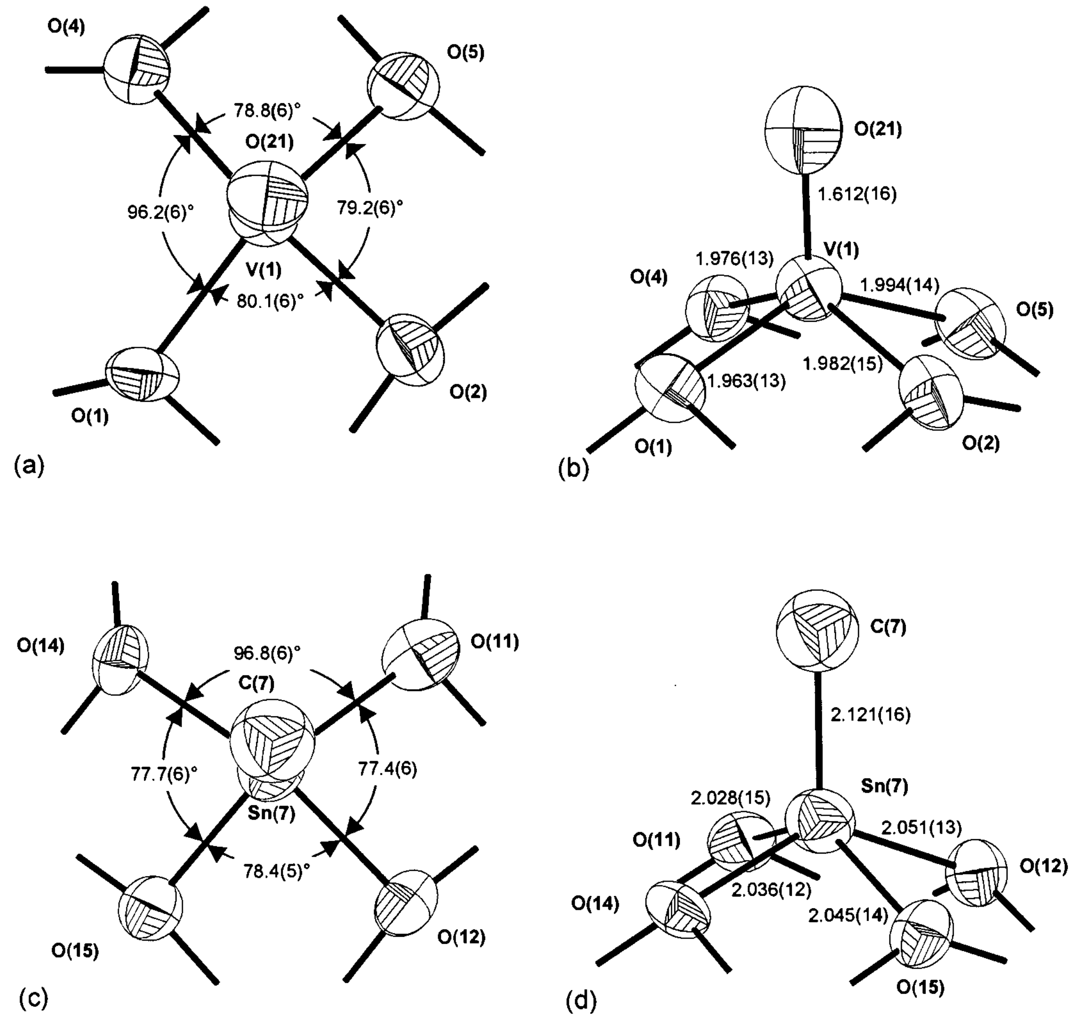

Fig. 3. Bond lengths and angles around V(1) (a, b) and Sn(7) (c, d) showing the similarities between square-pyramidally coordinated tin and vanadium atoms.

distorted icosahedron. The V–Sn distances lie in the range 3.093–3.757 Å, the Sn–Sn distances in the range 3.191–3.842 Å. In comparison to the $[(^{i}\mathrm{PrSn})_{12}\mathrm{O}_{14}(\mathrm{OH})_6]^{2+}$ ion, one of the square-pyramidal $\{^{i}\mathrm{PrSnO}_4\}$ groups in the central ring has been substituted by a square-pyramidal $\{\mathrm{OVO}_4\}$ group. In spite of this substitution, the basic metal–oxygen skeleton of the cage ion remains unchanged. As one $[^{i}\mathrm{PrSn}]^{3+}$ group is replaced by a $[\mathrm{VO}]^{2+}$ group, the charge of the cage cation is lowered from +2 to +1 and only one Cl^- anion is observed in the crystal structure.

The similarity between the square-pyramidal $\{\mathrm{OVO}_4\}$ group and a square-pyramidal $\{\mathrm{RSnO}_4\}$ group is shown in Fig. 3. In summary, the $\{\mathrm{OVO}_4\}$ group shows shorter metal–oxygen$_{\mathrm{basal}}$ bonds than the $\{^{i}\mathrm{PrSnO}_4\}$ groups in the central ring ($d_{\mathrm{V-O}} = 1.963–1.994$ Å, $\bar{d}_{\mathrm{V-O}} = 1.979$ Å, $d_{\mathrm{Sn-O}} = 1.992–2.135$ Å, $\bar{d}_{\mathrm{Sn-O}} = 2.049$ Å), the V–O$_{\mathrm{apical}}$ distance is 1.612(16) Å. A calculation of V–O bond valences [15,16] around V(1) gave a valence sum of +3.956 for the vanadium atom, which is in excellent agreement with V^{IV}.

The crystal structure is stabilized by a system of hydrogen bonds. Each cage ion is linked through two of its μ_2-OH groups by O(6)···Cl(1)···O(16) hydrogen bonds ($d_{\mathrm{O(6)-Cl(1)}} = 3.01(2)$ Å, $d_{\mathrm{O(16)-Cl(1)}} = 3.03(2)$ Å) to two neighbouring cage ions forming chains along the *a* axis. Furthermore, two of these chains are linked by hydrogen bonds from O(20) to O(21) ($d_{\mathrm{O(20)-O(21)}} = 2.69(2)$ Å), the oxygen atom of the oxovanadium group of another symmetry equivalent molecule. In effect, this leads to a hydrogen-bonded band structure (see Fig. 4).

The water molecule acts as donor and receptor of two hydrogen bonds, respectively. It receives two hydrogen bonds from O(3) and O(10) ($d_{\mathrm{O(3)-O(500)}} = 2.96(3)$ Å, $d_{\mathrm{O(10)-O(500)}} = 2.99(3)$ Å) and donates hydrogen bonds to Cl(1) and O(300), the oxygen atom of a

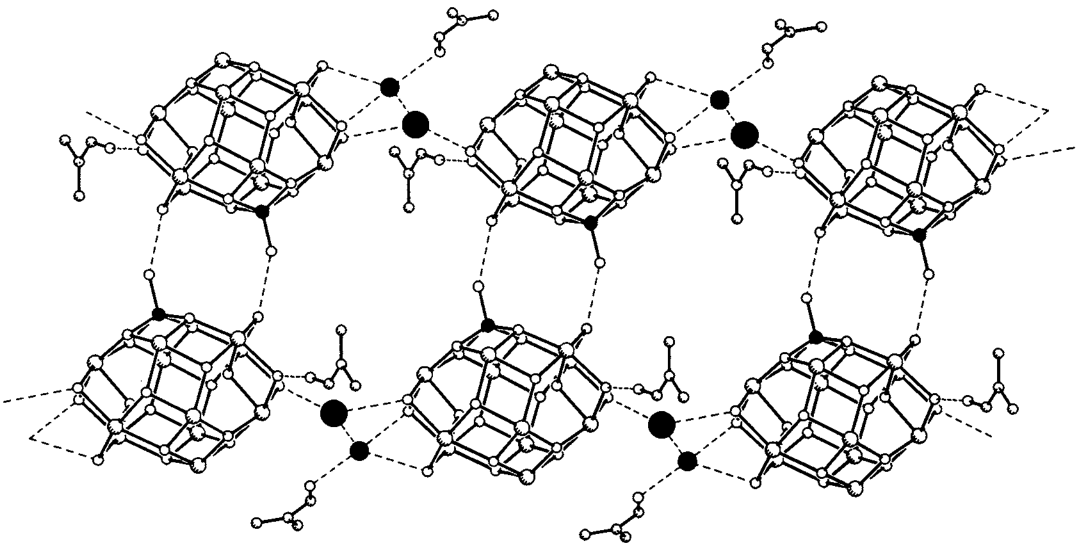

Fig. 4. Hydrogen bond system of **1** showing the Cl bridging, solvent molecules and the band structure. Tin: light shading; vandium: small black circles; carbon, oxygen, nitrogen: small open circles; chlorine: large black circle; oxygen (water): medium-sized black circle.

DMF molecule ($d_{O(500)-Cl(1)} = 2.98(2)$ Å, $d_{O(500)-O(300)} = 2.66(4)$ Å). The remaining μ_2-OH group, O(13), forms a hydrogen bond to O(300), the oxygen atom of the second DMF molecule ($d_{O(13)-O(200)} = 2.70(3)$ Å). No additional hydrogen bonds are observed between two neighbouring bands.

The composition of these crystals suggests that they are formed in accordance with Eq. (1):

$$\begin{aligned} &11\,{}^{i}\mathrm{PrSn(OH)_2Cl{\cdot}0.75H_2O} \\ &+ \mathrm{VOSO_4{\cdot}5H_2O} \xrightarrow{\mathrm{DMF/H_2O/En}} \mathbf{1}{\cdot}\mathrm{Cl{\cdot}2DMF{\cdot}H_2O} \\ &+ 5\ \mathrm{H_3N(CH_2)_2NH_3Cl_2} + \mathrm{H_3N(CH_2)_2NH_3SO_4} \\ &+ 4.5\mathrm{H_2O} \end{aligned} \tag{1}$$

However, the excess of $[VO]^{2+}$ described in Section 2 is necessary for the crystallization of **1**·Cl·2DMF·H$_2$O. Other conditions give rise to the separation of other crystals with other cations containing more VO groups but nevertheless an icosahedral metal arrangement. Therefore, it seems possible that in solution a time-, solvent-, salt- and temperature-dependent equilibrium between different cations exists. This interesting feature will be subject to NMR studies. With respect to the solution equilibrium, the crystals which separate are those that show the lowest solubility under the experimental conditions.

4. Supplementary material

Crystallographic data for the structural analysis reported in this paper have been deposited with the Cambridge Crystallographic Data Centre, CCDC no. 133227 for compound **1**·Cl·2DMF·H$_2$O. Copies of this information may be obtained free of charge from The Director, CCDC, 12 Union Road, Cambridge CB2 1EZ, UK (Fax: +44-1223-336033; e-mail: deposit@ccdc.cam.ac.uk or www: http://www.ccdc.cam.ac.uk).

Acknowledgements

The authors gratefully acknowledge financial support from the Fonds der Chemischen Industrie.

References

[1] M.T. Pope, A. Müller ((eds), Topics in Molecular Organization and Engineering. Polyoxometalates: From Platonic Solids to Anti-Retroviral Activity, vol. 10, Kluwer, Dordrecht, 1994.
[2] K.-H. Tykto, Chem. i. u. Z. 13 (1979) 184.
[3] H. Puff, H. Reuter, J. Organomet. Chem. 373 (1989) 173.
[4] D. Dakternieks, H. Zhu, J. Organomet. Chem. 476 (1994) 33.
[5] F. Banse, F. Ribot, P. Tolédano, J. Maquet, C. Sanchez, Inorg. Chem. 34 (1995) 6371.
[6] C. Eychenne-Baron, F. Ribot, C. Sanchez, J. Organomet. Chem. 567 (1998) 137.
[7] H. Reuter, Angew. Chem. 103 (1991) 1487.
[8] G.S. Chorghade, M.T. Pope, J. Am. Chem. Soc. 109 (1987) 5134.
[9] F. Xin, M.T. Pope, Inorg. Chem. 35 (1996) 1207.
[10] B. Krebs, B. Lettmann, H. Pohlmann, H. Fröhlich, Z. Krist. 196 (1991) 231.
[11] Y. Sasaki, H. Imoto, O. Nagano, Bull. Chem. Soc. Jpn. 57 (1984) 1417–1418.

[12] U. Behrens, A.K. Brimah, K. Yünlü, R.D. Fischer, Angew. Chem. 105 (1993) 117–119.
[13] A. Müller, R. Rohlfing, E. Krickemeyer, H. Bögge, Angew. Chem. 105 (1993) 916–918.
[14] G.M. Sheldrick, Program Package SHELXTL, Release 5.1, Siemens Analytical X-Ray Instruments Inc, Madison, WI, USA, 1997.
[15] I.D. Brown, D. Altermatt, Acta Crystallogr. B41 (1985) 244.
[16] N.E. Brese, M. O'Keefe, Acta Crystallogr. B47 (1991) 192.